

TABLE I  
SWITCH DESIGN PARAMETERS AND MEASURED PERFORMANCE

Quantity	Value
$f_0$ [Eq. (6)]	2295 MHz
VSWR [Eq. (1)]	1.065
$\epsilon$ [Eq. (6)]	14.5
$Y_0$ [Eq. (12)–(15)]	0.02 mho
$d$ [Input to Fig. 3]	0.3175 cm
$\kappa/\mu$ (Fig. 3)	0.51
$R$ (Fig. 3)*	1.18 cm
$Y_T$ (Fig. 3)	0.042 mho
$G_R$ (Fig. 3)	0.085 mho
bandwidth (Fig. 3)	18.5%
$f_0$ (measured)	2440 MHz
25-db return loss bandwidth (measured)	16%
25-db isolation bandwidth (measured)	12%
0.15-db insertion loss bandwidth (measured)	18%

\* The saturation magnetization of the ferrite ( $4\pi M_s$ ) is 680 gauss and the disks were mounted in stripline boards of dielectric constant 2.47.

Two facts should be noted regarding Fig. 3. The value of  $\kappa/\mu$  useful for design purposes is in the range 0.25 to 0.5, which limits the bandwidth range to 10–20 percent. Fig. 3 can also be used to design a switch for a given bandwidth. In this case, a vertical line is first drawn to cut the horizontal axis at the desired bandwidth value. The switch design and measured performance are summarized in Table I. The measured values were obtained after initial switch assembly, with no circuit optimization except adjusting the coil current of the magnetic circuit.

#### IV. CONCLUSIONS

A general design procedure for stripline  $Y$ -junction circulators has been presented. Computer evaluation of the resonator design and impedance matching enables the circulator to be characterized over the entire practical bandwidth range. The circulator can be designed from either a specified bandwidth or ground plane spacing. For the latter case, it avoids the need for multiple iterations using the resonator equations/Smith chart matching technique in [1] until a ferrite cylinder height is obtained to match the ground plane spacing. The experimental circulator is in good agreement with the calculated design values. Broader bandwidth and lower insertion loss have been demonstrated than that of the currently used switches employing extensive tuning procedures.

#### REFERENCES

[1] C. E. Fay and R. L. Comstock, "Operation of the ferrite junction circulator," *IEEE Trans. Microwave Theory Tech.*, vol. MTT-13, pp. 15–27, Jan. 1965.

#### A Quasi-Optical Single Sideband Filter Employing a Semiconfocal Resonator

PAUL F. GOLDSMITH AND HOWARD SCHLOSSBERG

**Abstract**—We describe a single sideband filter designed to have low insertion loss when used with microwave radiometer systems incorporating a feedhorn of relatively large beam divergence angle. The device we discuss is a type of Fabry–Perot interferometer employing one plane and one spherical mirror which form a near semiconfocal resonant cavity. Measurements on a prototype device operating at  $\nu \sim 100$  GHz with a  $f/D \sim 4$  feedhorn and a 1.4-GHz IF frequency are presented.

#### I. INTRODUCTION

Receiver systems employing mixers intended for reception of narrow-band signals (including most millimeter radioastronomical applications, for example) can advantageously use a low-loss single sideband input filter. The benefits are a significant reduction in the uncertainties concerning the atmospheric transmission and relative system gain in the two mixer sidebands [1]. The atmospheric absorption is generally inferred from its broadband (double sideband) emission which, however, can vary quite rapidly with frequency; the attenuation in either individual sideband is difficult to determine directly [2]. At millimeter wavelengths, low-loss easily tunable filters are most easily realized in a free space "quasi-optical" configuration rather than in waveguide. Systems utilizing Fabry–Perot resonators for single sideband filtering have been restricted to those with a large-diameter well-collimated beam [3]. Relatively few radio astronomical feed systems incorporate appropriate optics; in most cases the formation of the desired beam requires additional focusing optics [1]. The restrictions on beam diameter imposed by the requirement of low loss have been analyzed for a Gaussian beam incident on an infinite plane-parallel Fabry–Perot resonator [4]. The incident field distribution is of the form

$$P(r) = P(0) e^{-[r/w(z)]^2} \quad (1)$$

where  $w$  is the beam radius perpendicular to the direction of propagation and  $z$  is the distance along the axis of propagation measured from the location of the beam waist, where the beam radius attains its minimum size  $w_0$ . In this case, the fraction of the incident power transmitted at resonance is given approximately by the expression [4]

$$f_t \simeq 1 - \frac{1}{2} \left[ \frac{2\lambda d \cos \theta}{\pi w_0^2 T} \right]^2 \quad (2)$$

where  $\lambda$  is the wavelength of the signal,  $d$  the mirror separation,  $\theta$  the angle from normal incidence, and  $T$  the power transmission of a single mirror. For optimum single sideband filtering ( $\nu_{\text{IMAGE}}$  located halfway between two successive resonances)  $d = \lambda_{\text{IF}}/8$  and assuming normal incidence we find that to obtain  $f_t = 0.9$ ,  $w_0 = 0.42 \sqrt{\lambda \lambda_{\text{IF}}/T}$ . A mirror transmission of  $\sim 0.15$  is desirable for efficient filtering (see below and reference 1) so

Manuscript received January 9, 1980; revised June 12, 1980. This work was partially supported by the National Science Foundation under Grant 76-24610 and is contribution number 375 of the Five College Radio Astronomy Observatory.

P. F. Goldsmith is with Department of Physics and Astronomy and Department of Electrical and Computer Engineering, University of Massachusetts, Amherst, MA 01003.

H. Schlossberg is with the Physics and Geophysics Directorate, Air Force Office of Scientific Research (AFSC), Bolling AFB, Washington, D.C. 20332.

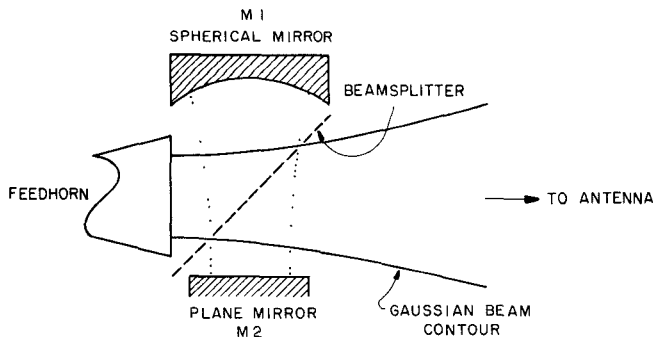


Fig. 1. Schematic drawing of the semiconfocal single sideband filter. The prototype model utilizes a mylar beamsplitter and a dual-mode feedhorn which has its beam waist near the horn aperture. The radius of curvature of the spherical mirror is 15 cm and the separation between the mirrors is 4-6 cm.

that for  $\lambda = 0.3$  cm and  $\lambda_{IF} = 20$  cm we require a beam waist radius of 2.7 cm. The beam diameter will depend on the level at which the beam is truncated but will typically be approximately  $3w_0$ . The resulting value is 8 cm; the equivalent  $f/D$  ratio which for a Gaussian beam is given approximately by  $w_0/\lambda$  is seen to be restricted to be equal to 9 for a transmission of 90 percent. Since the majority of existing systems do not use such large  $f/D$  systems, a filter capable of low loss with a smaller waist size is required; one such device is described below.

## II. RESONATOR DESIGN

Resonators incorporating focusing elements can have low loss because the beam is refocused after each reflection thus reducing the effect of diffraction. Fabry-Perot resonators incorporating spherical mirrors and having extremely high  $Q$  have been used in spectroscopy for some time [5], [6]; devices designed for this purpose have input and output coupling arrangements that are unsuitable for the present application. The device shown in Fig. 1 has several attractive features. We will describe its principle of operation in terms of a fundamental Gaussian beam (1) launched by the feedhorn. The feed system for the 14-m Five College Radio Astronomy Observatory<sup>1</sup> millimeter antenna employs a dual mode feedhorn [7] with aperture diameter 2.4 cm. The radiated pattern is very close to a Gaussian to a level  $\sim 17$  dB below the peak and from the measured pattern we determine a beam waist radius  $w_0 = 0.78$  cm. For this type of horn the waist location is very close to the aperture and the beam radius  $w$  and radius of curvature  $R$  are given by

$$w(z) = \left[ w_0^2 + \left( \frac{\lambda z}{\pi w_0} \right)^2 \right]^{1/2} \quad (3a)$$

$$R(z) = z + \frac{1}{z} \left( \frac{\pi w_0^2}{\lambda} \right)^2 \quad (3b)$$

where  $z$  is the distance from the horn aperture [8]. The spherical mirror M1 and the plane mirror M2 form a resonant cavity; if the mirror separation is  $d$  and the radius of curvature of the spherical mirror  $r$ , then the beam waist radius of the resonator is given by [8]

$$w_0' = \sqrt{\frac{\lambda}{\pi}} \left[ \frac{d}{\rho} \left( 1 - \frac{d}{\rho} \right) \right]^{1/4}. \quad (4)$$

For the case  $\rho = 2d$  the waist (located at the plane mirror) is of

<sup>1</sup>The Five College Radio Astronomy Observatory is operated with support from the National Science Foundation.

minimum size

$$w_0' = \sqrt{\frac{\lambda \rho}{2\pi}} \quad (5)$$

this is called a half-confocal [9] or more commonly semiconfocal resonator. For different mirror curvatures the waist location and size will be different.<sup>2</sup> The semiconfocal resonator has the mirror curvature producing lowest loss. The curvature of M1 must match that of the beam a distance  $d$  from the waist (3b) yielding  $w_0' = \sqrt{\lambda d / \pi}$  which can also be obtained from (5) and the relationship between  $f$  and  $d$  for the semiconfocal resonator.

The loss due to diffraction of this resonator configuration has been extensively investigated. The computations are in general presented for the case of symmetric geometry (with identical mirrors); the quantity  $N = a^2 / \lambda d$ , where  $a$  is the mirror radius, determines the power loss per transit, given by [9]

$$\alpha \approx 16\pi^2 N e^{-4\pi N}. \quad (6)$$

For the semiconfocal resonator, the loss per pass is given by the same formula but with  $N^{\text{eff}} = a^2 / 2\lambda d$  where both spherical and plane mirrors are assumed to have a radius  $a$ . From these results we find that a resonator capable of discriminating between signal and image frequencies at  $\sim 100$  GHz separated by 2-3 GHz can be constructed for the feed system discussed previously, and having a loss per transit less than 0.001; the resulting total diffraction loss depends on the resolution desired but typically will be  $< 0.1$ , as discussed further below. This low value compared to that obtained with a resonator incorporating plane parallel mirrors indicates the advantage of incorporating focusing elements into the resonator.

The relatively low diffraction losses expected for the semiconfocal resonator indicate that its frequency response in the configuration of Fig. 1 can be calculated satisfactorily from geometrical optics with the fraction of the electric field lost per transit due to diffraction given by  $\alpha^{1/2}$ . If we let  $T$  be the fraction of power transmitted by the beam splitter than we find that the fraction of the incident power transmitted by the resonator is given by

$$\tau = \frac{(4\beta T / (1 - \beta T)^2) \sin^2(\phi/2) + T((1 - \beta) / (1 - \beta T))^2}{1 + (4\beta T / (1 - \beta T)^2) \sin^2(\phi/2)} \quad (7)$$

where  $\phi$  is the round trip phase shift through the resonator and  $\beta = 1 - \alpha^{1/2}$ . The frequencies of maximum transmission will be given by the expression

$$\nu = \frac{c}{2d} (q + g) \quad (8)$$

where  $q$  is an integer (the axial mode number) and  $g$  is a geometry-dependent constant which has the value  $5/4$  for the exactly semiconfocal case. The form of the transmission function (7) is seen to be identical to that of a normal Fabry-Perot resonator in reflection but with  $1 - T$  (the power reflection coefficient of the beam splitter) replacing  $T$ . The resonances thus result in a large fraction of the incident power being reflected. In our case the minimum transmission is  $\sim T((1 - \beta) / (1 - \beta T))^2$ , the maximum transmission is  $\sim 4T / (1 + T)^2$  and the spacing of the transmission minima is  $c/2d$ .

The choice of beam splitter transmission is a tradeoff between rejection bandwidth and maximum resonator transmission. The

<sup>2</sup>For the purpose of calculating the loss, the semiconfocal resonator is equivalent to a confocal resonator consisting of two spherical mirrors identical to M1 separated by a distance  $2d$  if the diffraction loss of the plane mirror can be neglected.

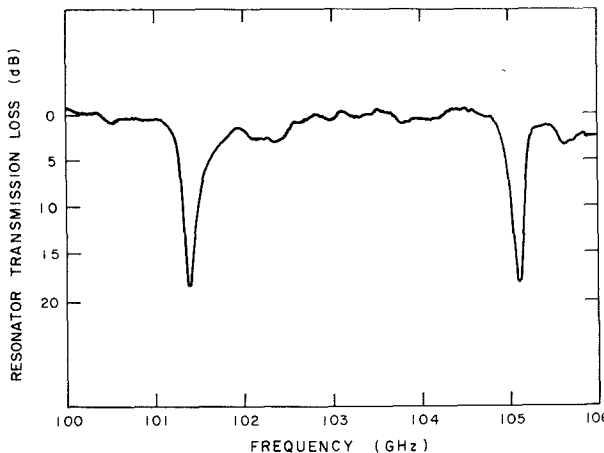


Fig. 2. Measured response of the resonator shown in Fig. 1 when used with the feedhorn described in the text. The response was determined by comparing the power collected by a small feedhorn located 15 cm from the resonator with and without the resonator in place. To reduce reflections, the feedhorn was covered with a  $\sim 1$ -cm thick sheet of Eccosorb (Emerson and Cuming, Inc., Canton, MA) having an attenuation of 5 dB.

intended use of this device is to suppress response at the unwanted image sideband while producing minimum attenuation at the frequency of the signal, separated from that of the image by  $2\nu_{IF}$  where  $\nu_{IF}$  is the IF frequency. In order to have minimum loss for the signal, the mirror spacing should be approximately  $\lambda_{IF}/8$  but for  $T > 0.7$  the theoretical transmission minimum is sharp enough that little additional signal loss is produced for a mirror spacing less than  $\lambda_{IF}/4$ . The bandwidth over which the resonator reflects power decreases as the transmission of the beamsplitter is increased; for  $T = 0.7$  the maximum theoretical transmission is 0.97 and the minimum transmission is more than 13 dB below the peak over a bandwidth equal to 10 percent of the IF frequency.

### III. PERFORMANCE MEASUREMENTS

The image rejection filter is designed to operate in the  $\lambda 0.3$ -cm– $0.25$ -cm range which covers several important astronomical spectral lines, and in which the atmospheric attenuation due to the 118-GHz  $O_2$  line is a rapidly varying function of frequency, making single sideband operation particularly desirable. The minimum mirror separation is 4 cm, due to mechanical constraints and the feedhorn size, which is acceptable though not optimal for use with the 1.4-GHz system IF frequency. The feedhorn beam waist radius together with the semiconfocal condition (4) then fixes the spherical mirror radius of curvature  $\rho$  to be 15 cm for  $\lambda = 0.26$  cm (the wavelength of the carbon monoxide  $J = 1 \rightarrow 0$  transition). We employ a dielectric beam splitter made of mylar; for a large set of measurements made at frequencies between 80 and 170 GHz we find that an index of refraction  $n = 1.75$  gives a good fit to the transmission of films of different thickness. A film 0.203 mm (0.008 in) thick is found to have  $T = 0.76$  at 100 GHz for an angle of incidence equal to  $45^\circ$ . The resonator transmission is measured with a backward-wave oscillator (BWO) sweeper and an isolated detector following a small (1-cm  $\times$  2-cm) feedhorn located on the axis of the receiver feedhorn, approximately 15 cm from the resonator. The response is shown in Fig. 2.

The main difficulty that arises when using this resonator is proper alignment—if the resonator is tilted or offset with respect to the correct axis, spurious modes can be excited resulting in low transmission at frequencies other than those of the funda-

mental mode resonances. Spurious modes appear to be the cause of the high frequency shoulder of the major responses seen in Fig. 2; these may be due in part to the non-Gaussian component of the feedhorn response pattern. Once the resonator has been properly aligned, it can be tuned between 80 and 110 GHz with no major change in the response pattern. With a feedhorn having a radiation pattern consisting essentially of a fundamental Gaussian mode, and after careful initial alignment, this device should be useful in a variety of applications. Due to the refocusing properties of the resonator neither the beam pattern nor the location of the feedhorn beam waist should be significantly affected.

We see from Fig. 2 that over much of the region between resonances the loss is less than 1 dB and the transmission drops below  $-10$  dB over a  $\sim 160$ -MHz bandwidth around the resonances. Since most of the power at the resonant frequency is reflected back into the feedhorn, this filter offers the possibility of making an image-enhanced mixer, although only over a very narrow bandwidth; this aspect of operation has not been investigated. The transmission minima derived from (6) and (7) are predicted to be between  $-23$  dB (for  $d = 6$  cm) and  $-47$  dB (for  $d = 5$  cm). The measured minimum transmission of  $\sim -17$  dB is essentially independent of mirror spacing which indicates that the loss per transit is dominated by coupling, ohmic, and dielectric losses, rather than by diffraction. If the entire loss at small spacings is due to these causes then we conclude that the sum of the field losses per transit  $\alpha_{\Omega}^{1/2} + \alpha_{COUPLING}^{1/2} + \alpha + \alpha_{DIEL}^{1/2} = 0.03$ . For equivalent beam and mirror parameters used in our system, a plane parallel resonator would have a diffraction loss per transit of 0.27, over 100 times greater than for the semiconfocal resonator, and would perform very poorly.

### IV. SUMMARY

We discuss the design of semiconfocal Fabry–Perot resonator designed for sideband filtering in divergent beams at millimeter wavelengths. The low diffraction loss of this type of resonator allows high signal transmission and good image rejection under conditions in which a plane parallel Fabry–Perot resonator would be excessively lossy. Measurements of the performance of a device designed for an IF frequency of 1.4 GHz and a  $f/D \sim 4.1$  beam are presented which are in reasonable agreement with the theory but the loss appears to be dominated by sources other than diffraction.

### ACKNOWLEDGMENT

The authors would like to acknowledge the hospitality of the Max-Planck-Institut für Radioastronomie, where the initial measurements of this device were carried out.

### REFERENCES

- [1] P. F. Goldsmith, "A quasioptical feed system for radioastronomical observations at millimeter wavelengths," *Bell Syst. Tech. J.*, vol. 56, p. 1483, Oct. 1977. (and references therein).
- [2] J. W. Waters, "Absorption and emission by atmospheric gases," in *Methods of Experimental Physics*, vol. 12, part B, M. L. Meeks, Ed. New York: Academic, 1976.
- [3] P. G. Wannier, J. A. Arnaud, F. A. Pelow, and A. A. M. Saleh, "Quasioptical band-rejection filter at 100 GHz," *Rev. Sci. Instrum.*, vol. 47, p. 56, Jan. 1976.
- [4] J. A. Arnaud, A. A. M. Saleh, and J. T. Ruscio, "Walk-off effects in Fabry–Perot dipoles," *IEEE Trans. Microwave Theory Tech.*, vol. MTT-22, p. 486, May 1974.
- [5] E. P. Valkenburg and V. E. Durr, "A high  $Q$  Fabry–Perot interferometer for water vapor absorption measurements in the 100 Gc/s to 300 Gc/s Frequency Range," *Proc. IEEE*, vol. 54, p. 493, Apr. 1966.
- [6] M. Lichtenstein, J. J. Gallagher, and R. E. Cupp, "Millimeter spectrome-

ter using a Fabry-Perot interferometer," *Rev. Sci. Instr.*, vol. 34, p. 843, Aug. 1963.

[7] P. D. Potter, "A new horn antenna with suppressed sidelobes and equal beamwidths," *Microwave J.*, vol. 6, p. 71, June 1963.

[8] H. Kogelnik and T. Li, "Laser beams and resonators," *Proc. IEEE*, vol. 54, p. 172, Oct. 1966.

[9] T. Li, "Diffraction loss and selection of modes in maser resonators with circular mirrors," *Bell Syst. Tech. J.*, vol. 44, p. 917, May-June 1965.

## Green's Functions for Triangular Segments in Planar Microwave Circuits

RAKESH CHADHA, STUDENT MEMBER, IEEE, AND  
K. C. GUPTA, SENIOR MEMBER, IEEE

**Abstract**—Green's functions are developed for the analysis of triangular segments in microwave planar circuits. Three types of triangles (30°–60° right-angled, equilateral, and isosceles right-angled) are treated by placing additional image sources outside the triangular region.

### I. INTRODUCTION

Two-dimensional microwave planar components have been proposed for use in microwave-integrated circuits [1]–[3]. One of the methods for analyzing these components is by use of Green's functions relating voltage at any point to a line current excitation [1]. The Green's functions for rectangular and circular geometries are available [1]. Recently triangular elements have also been proposed for realizing resonators and prototype elements for bandpass and bandstop filters [4], [5]. The triangular resonators have been used in the design of 3-port circulators [5], and gap-coupled triangular segments have been proposed for use in filter circuits [4]. Also, characterization of triangular segments is necessary when an accurate analysis of a three-microstrip junction (such as encountered in power dividers), shown in Fig. 1, is needed. However, Green's functions for triangular geometries have not been reported so far. This paper describes the development of Green's functions for three kinds of triangular geometries useful in planar circuits. These are 1) a 30°–60° right-angled triangle, 2) an equilateral triangle, and 3) an isosceles right-angled triangle.

The basic integral equation involved in the analysis of planar circuits [1] is

$$V(x, y) = \iint_D G(x, y | x_0, y_0) i(x_0, y_0) dx_0 dy_0 \quad (1)$$

where  $G$  is the Green's function of the second kind having dimension of impedance and  $i(x_0, y_0)$  denotes a fictitious source current density injected normally.  $V(x, y)$  denotes voltage at any point on the segment with respect to the ground plane. Equation (1) is satisfied inside the contour  $C$  (Fig. 2), and the open boundary condition on  $C$  may be written as

$$\frac{\partial V}{\partial n} = 0. \quad (2)$$

Manuscript received March 19, 1980; revised June 12, 1980. This work was supported by the Department of Electronics, Government of India, under a research grant.

The authors are with the Department of Electrical Engineering, Indian Institute of Technology, Kanpur 208016, India.

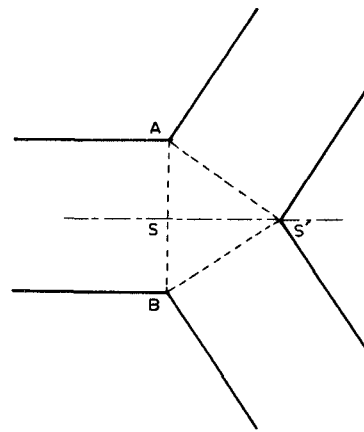


Fig. 1. Triangular segment in a typical  $Y$  junction.

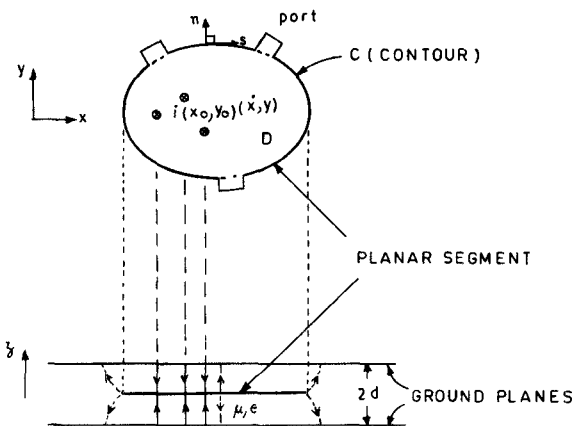


Fig. 2. Configuration for a typical segment in planar microwave circuits.

In planar circuits the dimension  $d$  is much smaller than the wavelength and the Green's function  $G$  is given by the solution of

$$(\nabla_T^2 + k^2)G = -j\omega\mu d\delta(x - x_0)\delta(y - y_0) \quad (3)$$

with

$$\frac{\partial G}{\partial n} = 0. \quad (4)$$

In the above,  $k$  denotes propagation constant ( $\omega\sqrt{\mu\epsilon}$ ) in the dielectric medium. Product of delta functions  $\delta(x - x_0)\delta(y - y_0)$  represents a line current flowing along  $z$ -direction and located at  $(x_0, y_0)$ . Such sources have been called line sources in the text later.

In circuits, which are symmetrical about an axis, even- and odd-symmetry can be used for complete analysis of the circuit. For example, in the circuit of Fig. 1, even- and odd-mode circuits may be analyzed separately. For the odd-mode circuits, the plane of symmetry ( $SS'$  in Fig. 1) is replaced by an electric wall at which the boundary condition

$$G = 0 \quad (5)$$

must be satisfied. Thus, there is a need to obtain odd-mode Green's functions, which satisfy (5) on one side of triangle ( $SS'$ ) and (4) on the remaining sides ( $AS$  and  $AS'$ ) of the planar segment. The function  $G$  is evaluated for different triangular geometries in the following sections.